とが示された．従ってここで用いた薬剤をウイルス不活化のための物理化学的淘汰圧と置き換えることにより，不活化に抵抗性のウイルスを分離し，その抵抗性を解析することでウイルス不活化のための条件を解明することができることが期待される．それによって不活化技術の開発につなげていけるものと考えられた．

（２）FCVの感染感受性と宿主域．

FCVは本来の宿主であるネコ細胞CR-FK細胞以外にアフリカミドリザル細胞CV-1, Vero細胞で感染性を示した．FCVは細胞表面のJAM1を感染レセプターとして細胞内に侵入する．そこでネコ，アフリカミドリザル，ヒトのJAM1のアミノ酸配列を比較した(図７)．ネコとアフリカミドリザルのJAM1の相同性は79.2%，アフリカミドリザルとヒトは96.3%，ヒトとネコは79.6%である．アフリカミドリザルとヒトのJAM1はアミノ酸残基が４つ異なっていることから，FCVがアフリカミドリザル細胞に感染の可否がレセプターのJAM1に依存するのだとすると，ウイルス複製に重要なアミノ残基は，アフリカミドリザルのAla^{7}, Ser^{90}, Lys^{154}, Ile^{253}であろうと推定される．どのアミノ酸残基が，FCVがCV-1やVero細胞への侵入に関与しているのかは，組み換えウイルスを使った実験によって明らかになると考えられる．

FCVは同じアフリカミドリザルの腎由来の細胞であるCV-1，Vero細胞に感染可能であったが，Vero細胞ではウイルスの継代はできなかった．この違いは，Vero細胞表面のJAM1の発現レベルが低いからであるという可能性と，Vero細胞では感染侵入後の細胞内での複製過程に阻害因子がある可能性，あるいは複製に必要な因子を欠いている可能性，あるいは必要な因子が十分に発現していない可能性が考えられる．この点を解析するためには，CV-1とVero細胞表面のJAM1分子の発現レベルを比較する必要がある．また細胞侵入後にVero細胞に必要な因子がないのか，阻害因子があるかは，CV-1細胞とVero細胞の融合細胞にFCVが感染複製するかどうかを調べる必要がある．

（２）FCVの他種動物細胞への馴化．

FCVはCV-1細胞により継代することにより，わずか３回の継代でCV-1細胞に馴化し，CR-FK細胞並みに複製能を高めることがわかった．これはカリシウイルスが，いかに宿主に馴化し易いかを示したものである．この変化が感染侵入時のレセプターとの相互作用に起きているとすると，FCVのカプシドタンパク質であるVP1にアミノ酸変異を起こしている可能性が高く，この解析も必要になってくる．

RNAウイルスはそのポリメレースのfidelityが低いため，変異ウイルスが出現し易いことが知られている．2008, 2009年に医薬品製造リアクター汚染を引き起こしたvesivirus 2117は，FCVと近縁のウイルスであるが，このウイルスの自然宿主は不明な

ままである．本来vesivirus 2117はヒトと接触のある自然宿主から医薬品製造に関わるヒトを介してCHO細胞を汚染したものと考えられているが，今回の実験によってFCVも医薬品製造用細胞を汚染する可能性がある．これを明らかにするためには，薬品製造用細胞に感染可能な変異ウイルスがどのような頻度で出現するのかについて実験的に推定する必要がある．

一方，アフリカミドリザルのレセプターの構造はヒトのものと96.3%の相同性をもつことから，アフリカミドリザルに馴化したウイルスはヒト細胞に感染可能である可能性が考えられた．しかしアフリカミドリザル細胞とヒト細胞の共培養によって，ヒト感染カリシウイルスの出現は起きなかった．このことはヒト細胞への感染にはアフリカミドリザルに比べて高い種の壁が存在することを示唆している．

E. 結論

今回得られたウイルスクローンからなるウイルス集団は，gp120のV3領域のみに多様な変異をもつ他は均一のウイルスライブラリーである．V3に多様な変異の組み合わせをもつウイルス集団であり，ウイルス不活化に対し，異なる反応性を持つことが予想される．今後は，温度，界面活性剤，pHなどのウイルス不活化過程に多様な変異gp120がどのような影響をもつのかを明らかにする予定である．

FCVはノロウイルスと近縁であるため，ノロウイルスの代替ウイルスとして使われることがあるが，血液製剤や組み換えタンパク質製造におけるモデルウイルスとしても有用であると考えられる．本研究ではFCVの宿主域を調べ，アフリカミドリザル腎由来細胞にも感染することが明らかになった．アフリカミドリザルの腎由来細胞はワクチン製造などにも多用される細胞であり，その点からもモデルウイルスの宿主域の解析は重要であると考えられる．

F. 健康危険情報

なし

G. 研究発表

1. 論文発表

(1) Maeda, Y., Yusa, K., Nakano, Y., Harada, S. Involvement of inhibitory factors in the inefficient entry of HIV-1 into the human CD4 positive HUT78 cell line. *Virus Res.* 155: 368-371, 2011.

(2) Yuan, Y., Maeda, Y., Terasawa, H., Monde, K., Harada, S., Yusa, K. A Combination of Polymorphic Mutations in V3 Loop of HIV-1 gp120 Can Confer Noncompetitive Resistance to Maraviroc. *Virology,* 413:293-299, 2011.

(3) Maeda, Y., Yoshimura, K., Miyamoto, F., Kodama, E., Harada, S., Yuan, Y., Harada, S., Yusa, K. *In vitro* and *In vivo* Resistance to Human Immunodeficiency Virus Type 1 Entry Inhibitors. *J. AIDS Clin. Res.* S2-004, 2011.

(4) 遊佐敬介, 山口照英, 川崎ナナ.
ヒトに感染が疑われているレトロウイルスとウイルス安全性, 医薬品医療機器レギュラトリーサイエンス 42: 444-447, 2011.

(5) 遊佐敬介, 新見伸吾, 橋井則貴. バイオ医薬品の外来性感染物質について *Pharm. Tech. Jpn. in press.*

2. 学会発表

(1) Yuan, Y., Maeda, Y., Hiromi, T., Monde, K., Yusa, K., Harada, S. Complete resistance to maraviroc in R5 HIV-1 with gp120 V3 loop mutations is affected by T199K and/or T275M in Env. 11th KUMAMOTO AIDS Seminar - GCOE Joint International Symposium, Aso, 10.6.2010. (2) 前田洋助, 中野雄介, 遊佐敬介, 原田信志. HIV-1 侵入過程のビリオン動態の可視化. 第58回に本ウイルス学会学術集会 徳島; 11.9.2010.

(3) 遊佐敬介, Yuan Yuzhe, 前田洋助, 寺沢広美, 門出和精, 原田信志. HIV-1 の gp120 V3 ループ変異による侵入阻害剤Maraviroc高度耐性の獲得. 第58回に本ウイルス学会学術集会 徳島; 11.9.2010.

(4) 中野雄介, 前田洋助, 遊佐敬介, 原田信志. コレセプター阻害剤によるコレセプター間oligomerization修飾. 第24回日本エイズ学会学術総会 東京 11.24.2010; 2010.

(5) 遊佐敬介, Yuan Yuzhe, 前田洋助, 寺沢広美, 門出和精, 原田信志. HIV-1 の gp120 V3 ループ変異による侵入阻害剤Maraviroc高度耐性の獲得. 第24回日本エイズ学会学術集会 東京 11.25. 2010.

(6) Yusa, K., Yuan, Y., Maeda, Y., Hiromi, T., Monde, K., Harada, S. A Combination of Polymorphic Mutations in V3 Loop of HIV-1 gp120 Can Confer Noncompetitive Resistance to Maraviroc. *International Union of Microbiological Societies, XV, International Congress of Virology*, Sapporo, September 2011.

(7)原田恵嘉, 濱治有希, 遊佐敬介, 松下修三, 吉村和久.抗HIV剤がEnv多様性に与える影響. 第25回日本エイズ学会学術総会 東京 11.30.2011.

(8) 中野雄介, 前田洋助, 遊佐敬介, 原田信志. コレセプター阻害剤によるCCR5のoligomerization 増強に関与するCCR5領域の解析. 第25回日本エイズ学会学術総会 東京 11.30.2011.

H. 知的財産権の出願・登録状況

なし

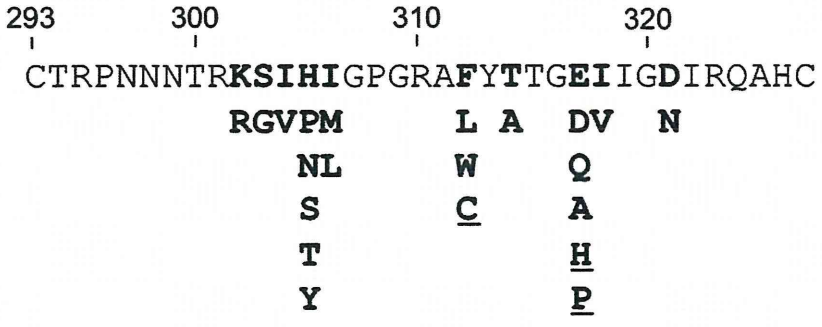

図1　ヒトレトロウイルスエンベロープタンパク質のV3 部分にpolymorphicなアミノ酸置換を導入し, V3に関するウイルスライブラリーを作製した. この領域は. 標的細胞への侵入時にコレセプターと相互作用する.

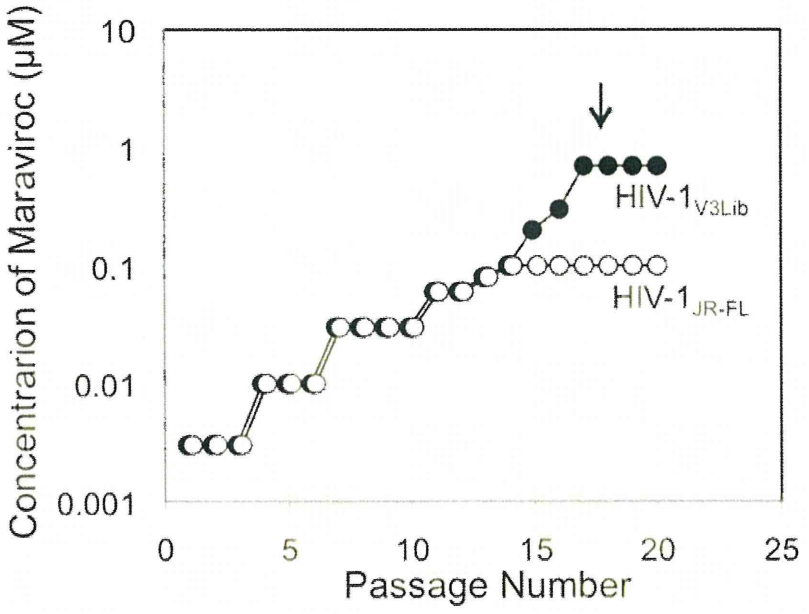

図2　ここでは選択圧として薬剤を使い, 特異的なV3構造をもつウイルスが選ばれてくるかどうかを調べた. 野生株に比べて, ライブラリーウイルスからは、薬剤に強い抵抗性をもつウイルスが, 選択されてくることがわかる.

表１　　選択されたウイルスの薬剤感受性を調べると抵抗性を示した.

	EC_{50}[a] (μM)	
	maraviroc[b]	TAK-779[b]
$HIV\text{-}1_{JR\text{-}FL}$	0.0069 ± 0.0019[c] (1.0)	0.043 ± 0.009 (1)
$HIV\text{-}1_{JR\text{-}FL\text{-}p17}$	0.055 ± 0.0055 (8)	0.15 ± 0.033 (3.5)
$HIV\text{-}1_{V3Lib}$	0.0055 ± 0.0007 (0.8)	0.025 ± 0.007 (0.6)
$HIV\text{-}1_{V3Lib\text{-}p17}$	> 10 (> 1449)	> 10 (> 233)

[a] PM1/CCR5 cells were infected at 100 $TCID_{50}$ in the presence of the CCR5 inhibitor on day 0. Cytopathic effect was determined on day 6 by the MTT method.
[b] Drug concentrations of 50% growth inhibition of the cells (CC_{50}) was > 10 μM.
[c] mean ± SD (n = 3).

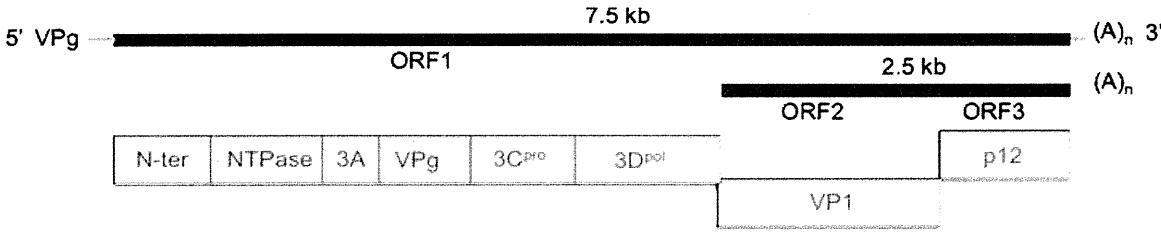

図３　FCV のゲノム構造とウイルスタンパク質

表２　細胞のFCV感受性（$TCID_{50}$）

cells / virus	HeLa	293T	Jurkat	Vero	CV-1	NIH-3T3	CR-FK
poliovirus	$10^{6.7}$	$10^{6.0}$	<1	$10^{7.3}$	$10^{6.0}$	<1	<1
sindbis virus	ND	$10^{6.7}$	<1	$10^{7.5}$	$10^{6.7}$	$10^{5.0}$	$10^{8.1}$
FCV	<1	<1	<1	$10^{4.0}$	$10^{3.7}$	<1	$10^{8.5}$

*ND, not determined.

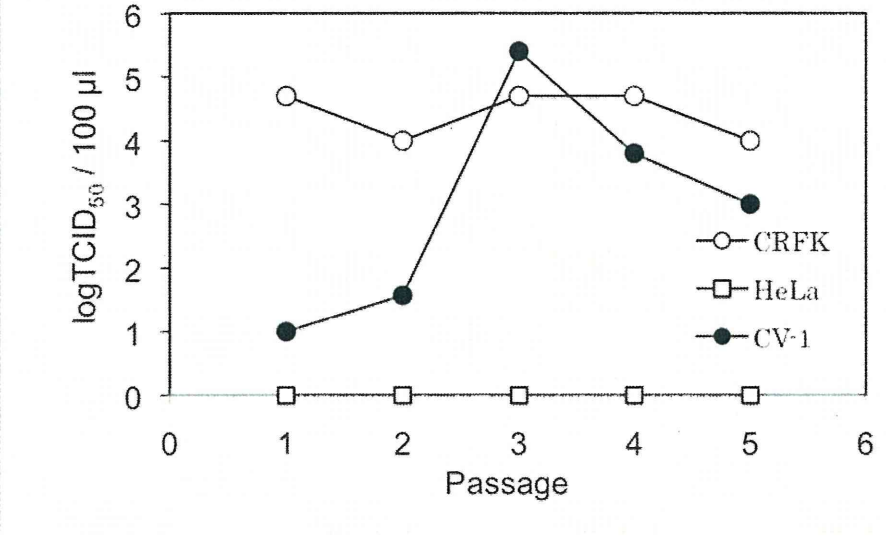

図４　CV-1細胞による継代によるFCV の馴化

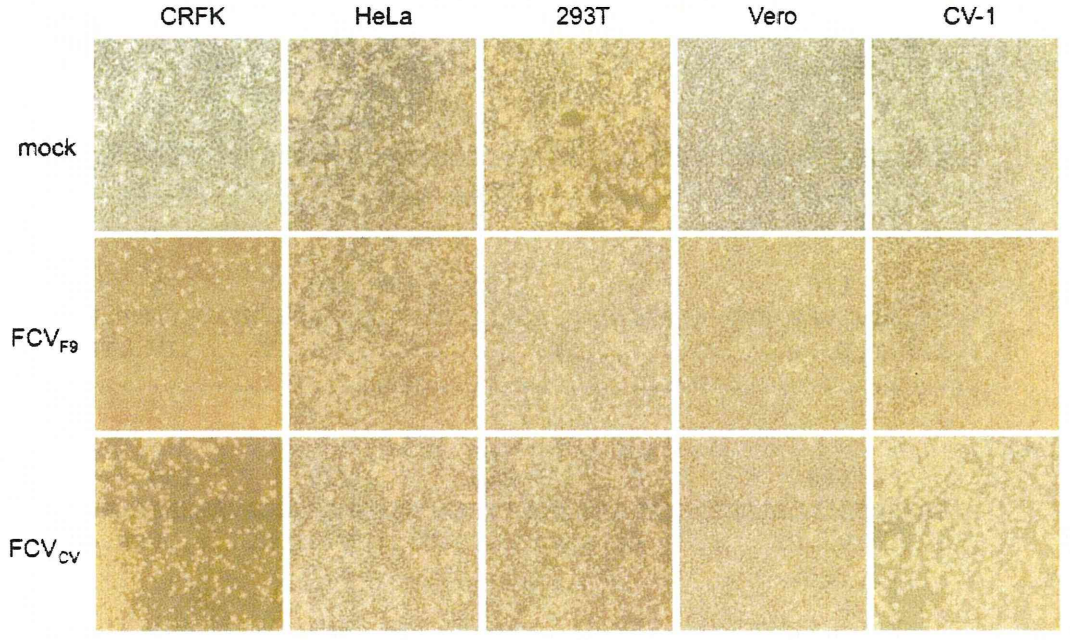

図５　分離したFCV$_{CV}$ はCV-1細胞に感染し，強い細胞変性を引き起こす

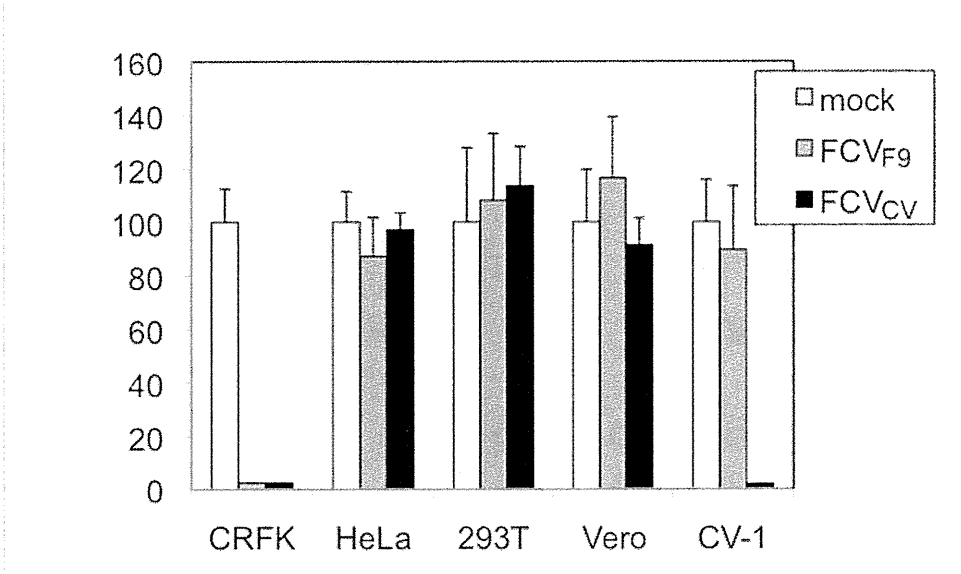

図６　FCV_{CV} はCV-1細胞にのみ強い細胞変性を引き起こす

```
        1         10         20         30         40         50         60
feline  MGTEARAGRRQLLVFT-SVVLSSLALGRGAVYTSEPDVRVPEDKPAKLSCSYSGFSNPRV
AGM     ...K.QAD.KL.HL..LAIL.CP....SVT.HS...E..I..NN.V....A.....S...
human   ......VE....C.........S.....................................

                70         80         90        100        110        120
        EWKFAHGDITSLVCYKNKITASYADRVTFSHSGITFHSVTRKDTGTYTCMVSDDGGNTYG
        ....DQ..T.K....N.......E.....LPS....K....E..........EE...N..
        ..........R.....................T.........................S..

                130        140        150        160        170        180
        EVSVQLTVLVPPSKPTVHIPSSATIGSRAVLTCSEKDGSPPSEYYWFKDGVRMPLEPKGN
        ..K.K.I.L........S........N........K........T.....IV..TN..ST
        ..................N..................Q.........................


                190        200        210        220        230        240
        RAFSNSSYSLNEKTGELVFDPVSAWDTGEYTCEAQNGYGMPMRSEAVRMEAAELNVGGIV
        ........V..PT........L..S.....S...R....T..T.N......VER...V..
        ............................................................


                250        260        270        280        290
        AAVLVTLILLGFLILGIWFAYRRGYFDRTKKGTSSKKVIYSQPAARSEGEFRQTSSFL-
        ...........I.IF......S..H..................S.......K......V
                     V                                S
```

図７　ネコ，アフリカミドリザル，ヒトの JAM1 のアミノ酸配列の比較

研究成果の刊行に関する一覧表

書籍

著者氏名	論文タイトル名	書籍全体の編集者名	書籍名	出版社名	出版地	出版年	ページ
Takao Hayakawa, Akiko Ishii-Watabe	Japanese Regulatory Perspective on Immunogenicity.	Michael Tovey.	Detection and Quantification of Antibodies to Biopharmaceuticals	John Wiley & Sons Inc.,	New Jersey, USA	2011	57-80

雑誌

発表者氏名	論文タイトル名	発表誌名	巻号	ページ	出版年
橋井則貴，原園　景，川崎ナナ	バイオ医薬品の物理的化学的性質解析の現状	ﾌｧｰﾑﾃｸ ｼﾞｬﾊﾟﾝ	27(13)	99-104	2011
山口照英，石井明子	早期臨床開発段階でのバイオ医薬品の品質・安全性確保	臨床評価	36	611-627	2009
Maeda, Y., Yusa, K., Nakano, Y., Harada, S.	Involvement of inhibitory factors in the inefficient entry of HIV-1 into the human CD4 positive HUT78 cell line.	Virus Res.	155	368-371	2011
Yuan, Y., Maeda, Y., Terasawa, H., Monde, K., Harada, S., Yusa, K.	A Combination of Polymorphic Mutations in V3 Loop of HIV-1 gp120 Can Confer Noncompetitive Resistance to Maraviroc.	*Virology*	413	293-299	2011
Maeda, Y., Yoshimura, K., Miyamoto, F., Kodama, E., Harada, S., Yuan, Y., Harada, S., Yusa, K.	*In vitro* and *In vivo* Resistance to Human Immunodeficiency Virus Type 1 Entry Inhibitors.	*J. AIDS Clin. Res.*	S2	004	2011
遊佐敬介，山口照英，川崎ナナ	ヒトに感染が疑われているレトロウイルスとウイルス安全性	医薬品医療機器レギュラトリーサイエンス	42	444-447	2011
遊佐敬介，新見伸吾，橋井則貴	バイオ医薬品の外来性感染物質について	*Pharm. Tech. Jpn.*	28	941-946	2012

research articles Journal of proteome research

Identification of Glycoproteins Carrying a Target Glycan-Motif by Liquid Chromatography/Multiple-Stage Mass Spectrometry: Identification of Lewis x-Conjugated Glycoproteins in Mouse Kidney

Noritaka Hashii,[†,‡] Nana Kawasaki,[*,†,‡] Satsuki Itoh,[†] Yukari Nakajima,[†,‡] Akira Harazono,[†] Toru Kawanishi,[§] and Teruhide Yamaguchi[†]

Division of Biological Chemistry and Biologicals, National Institute of Health Sciences, 1-18-1 Kamiyouga, Setagaya-ku, Tokyo 158-8501, Japan, and Core Research for Evolutional Science and Technology (CREST) of the Japan Science and Technology Agency (JST), 4-1-8 Hon-cho, Kawaguchi, Saitama 332-0012 Japan

Received January 20, 2009

Certain glycan motifs in glycoproteins are involved in several biological events and diseases. To understand the roles of these motifs, a method is needed to identify the glycoproteins that carry them. We previously demonstrated that liquid chromatography−multiple-stage mass spectrometry (LC−MS^n) allowed for differentiation of oligosaccharides attached to Lewis-motifs, such as Lewis x (Le^x, Galβ1−4(Fucα1−3)GlcNAc) from other glycans. We successfully discriminated Le^x-conjugated oligosaccharides from other N-linked oligosaccharides derived from mouse kidney proteins by using Lewis-motif-distinctive ions, a deoxyhexose (dHex) + hexose (Hex) + *N*-acetylhexsosamine (HexNAc) fragment (*m/z* 512), and a Hex + HexNAc fragment (*m/z* 366). In the present study, we demonstrated that this method could be used to identify the Le^x-conjugated glycoproteins. All proteins in the mouse kidney were digested into peptides, and the fucosylated glycopeptides were enriched by lectin-affinity chromatography. The resulting fucosylated glycopeptides were subjected to two different runs of LC−MS^n using a Fourier- transform ion cyclotron resonance mass spectrometer (FTICR−MS) and an ion trap-type mass spectrometer. After the first run, we picked out product ion spectra of the expected Le^x-conjugated glycopeptides based on the presence of Lewis-motif-distinctive ions and assigned a peptide + HexNAc or peptide + (dHex)HexNAc fragment in each spectrum. Then the fucosylated glycopeptides were subjected to a second run in which the peptide-related fragments were set as precursor ions. We successfully identified γ-glutamyl transpeptidase 1 (γ-GTP1), low-density lipoprotein receptor-related protein 2 (LRP2), and a cubilin precursor as Le^x-conjugated glycoproteins by sequencing of 2−5 glycopeptides. In addition, it was deduced that cadherin 16, dipeptidase I, H-2 class I histocompatibility antigen, K−K alpha precursor (H2−K(k)), and alanyl (membrane) aminopeptidase could be Le^x-conjugated glycoproteins from the good agreement between the experimental and theoretical masses and fragment patterns. The results indicated that our method could be applicable for the identification and screening of glycoproteins carrying target glycan-motifs, such as Lewis epitopes.

Keywords: liquid chromatography/multiple-stage mass spectrometry • specific detection • database search analysis • Lewis x-conjugated oligosaccharides

Introduction

Glycosylation is one of the most common post-translational modifications of proteins.[1,2] Certain glycan motifs on glycoproteins are involved in several biological events, including cell adhesion,[3] differentiation and development. They are also known to be closely associated with some diseases, such as tumors and hepatic diseases.[4−6] Glycomics, the study of all glycoconjugates in a cell type or in an organism, is crucial to understanding the mechanisms of glycan-mediated biological events and diseases.[7,8] Mass spectrometry (MS) and multiple-stage mass spectrometry (MS^n) in combination with several types of chromatography are known to be the most powerful tools of structural glycomics.[9−14] There are two major approaches to mass spectrometric glycome analysis. One is mass spectrometric glycan profiling, which is achieved by online or off-line liquid chromatography/mass spectrometry (LC−MS) of oligosaccharides enzymatically or chemically released from proteins.[15−22] This technique has advantages for conducting a detailed structural analysis and a quantitative analysis of

* To whom correspondence should be addressed. Division of Biological Chemistry and Biologicals, National Institute of Health Sciences, 1-18-1 Kamiyouga, Setagaya-ku, Tokyo 158-8501, Japan. Fax: +81-3-3700-9084. E-mail: nana@nihs.go.jp.
† National Institute of Health Sciences.
‡ Japan Science and Technology Agency.
§ Division of Drugs, National Institute of Health Sciences.

10.1021/pr9000527 CCC: $40.75

oligosaccharides,[23-25] but it does not provide any information on protein sources that carry the glycans of interest. The other approach is the mass spectrometric mapping of proteolytic digests. This method enables us to characterize glycan structures based on fragment ions,[26-31] and to deduce the peptide sequence from b- and y-ions that arise from the peptide backbone.[27] In addition to these approaches, glycomics require more advanced methods that can identify target proteins carrying a glycan motif of interest; that is to say, a technique for focused glycomics.

Lectin and immunological-based approaches have been widely used for the specific detection of target glycans and glycoproteins.[32-34] There have been numerous reports on the use of MS in combination with affinity chromatography and Western blotting with lectins or glyco-epitope-specific antibodies.[35-38] In a previous study, we demonstrated that LC−MS^n is also useful for the analysis of target glycans in a complex mixture.[39] Several glycan motifs often yield motif-specific ions by MS^n, along with common glycan-related ions such as the *N*-acetylhexosamine (HexNAc) fragment (*m*/*z* 204) and hexose (Hex) + HexNAc fragment (*m*/*z* 366).[40,41] For example, Lewis-motifs that consist of fucose (Fuc), galactose (Gal) and *N*-acetylglucosamine (GlcNAc) yield a distinctive ion at *m*/*z* 512 that corresponds to the B-type ion of deoxyhexose (dHex) + Hex + HexNAc. This B-type ion subsequently provides the product ion at *m*/*z* 366 ([Hex + HexNAc]$^+$) by MS/MS/MS. Using these Lewis-motif-distinctive ions, we successfully differentiated the oligosaccharides bearing the Lewis-motifs from many other oligosaccharides in mouse kidneys.[39] This method could be used to differentiate the Lewis-conjugated glycopeptides from a proteolytic digestion of proteins. Furthermore, the protein sources of the Lewis-motif-conjugated glycopeptides could be identified by further MS^n of peptide-related ions.

In this study we demonstrated a method for the identification of Lewis x (Le^x, Galβ1−4(Fucα1−3)GlcNAc)-conjugated glycoproteins in tissue by LC−MS^n. Our method consists of two different runs of LC−MS^n using a Fourier-transform ion cyclotron resonance mass spectrometer (FTICR−MS) and ion trap-type mass spectrometer (IT-MS). After the first run, we sorted out the product ion spectra of expected Le^x-conjugated glycopeptides based on the presence of Lewis-motif-distinctive ions and assigned a peptide + HexNAc or peptide + (dHex-)HexNAc fragment in each spectrum. Then the fucosylated glycopeptides were subjected to a second run in which the peptide-related fragments were set as precursor ions (Figure 1). As a model tissue, we used a mouse kidney in which we previously confirmed the presence of the Galβ1−4(Fucα1−3)GlcNAc motif (Lewis x and y) as well as the absence of the Galβ1−3(Fucα1−4)GlcNAc motif (Lewis a and b) and Fucα1−2Galβ1−3/4GlcNAc motif (blood group H).[39]

Experimental Section

Materials. Trypsin (Trypsin Gold, mass spectrometry grade), *Aleuria aurantia* lectin (AAL)-immobilized agarose column and Peptide-*N*-glycosidase F (PNGase F) were purchased from Promega (Madison, WI), Honen (Tokyo, Japan) and Roche (Mannheim, Germany), respectively. Murine kidneys (MRL/MpJ-lpr/lpr) were purchased from Japan SLC Inc. (Hamamatsu, Japan).

Sample Preparation. Murine kidney cells were filtrated by a cell strainer (70 μm; BD Biosciences, San Jose, CA) and solubilized in lysis buffer (7 M urea, 2 M thiourea, 2% CHAPS, and 30 mM Tris-HCl) containing a protease inhibitor mixture (Wako, Tokyo, Japan) by vortexing at 4 °C. After quantifying the proteins, cold acetone (final concentration, 80%(v/v)) was added to the protein solution (500 μg protein). The precipitated protein was dissolved again in 100 μL of 0.5 M Tris-HCl, pH 7.0, and precipitated with an 8-fold volume of acetone. The precipitated protein was dissolved in 810 μL of 0.5 M Tris-HCl (pH 8.6) containing 8 M guanidine-HCl and 5 mM EDTA, and the mixture was incubated with 6.0 μL of 2-mercaptoethanol at room temperature for 2 h. Freshly prepared 0.6 M sodium monoiodoacetate (135 μL) was added to the solution, and the mixture was incubated at room temperature for 2 h in the dark. The reaction mixture was desalted with a PD10 column (GE Healthcare Bio-Sciences, Uppsala, Sweden), and the solution containing proteins was freeze-dried. The carboxymethylated proteins were dissolved in 500 μL of bicarbonate buffer (pH 8.5) and incubated with 2 μg of trypsin at 37 °C for 16 h. After deactivation of trypsin by boiling for 3 min, a 10-fold volume of phosphate buffered saline (PBS) was added to the reaction mixture.

Lectin Affinity Chromatography. The sample solution was applied to the AAL-immobilized agarose column (1.45 mg of lectin, 1.5 × 1.0 cm) and washed with 2.5 mL of cold PBS at 4 °C (approximately one drop/s). The absorbed glycopeptides were eluted with PBS containing 0.2 M fucose (2.5 mL), and the fraction was desalted with a C18 cartridge (Micro Trap, 8.0 × 1.0 mm; Michrom BioResources, Auburn, CA). The absorbed glycopeptides in the cartridge were eluted with 2 mL of 0.1% trifluoroacetic acid containing 45% acetonitrile, and the fraction was dried, resuspended in 0.1% formic acid, and then analyzed by LC−MS^n.

PNGase F Treatment. Fucosylated glycopeptides enriched by lectin affinity chromatography were treated with 10 units of PNGase F in 50 μL of 50 mM phosphate buffer (pH 8.0) at 37 °C for 48 h to release *N*-linked oligosaccharides. After terminating the reaction by boiling, the reaction mixture was evaporated to dryness, resuspended in 0.1% formic acid, and then analyzed by LC−MS/MS.

Online Liquid Chromatography/Mass Spectrometry (LC−MS). Chromatographic separation of the fucosylated glycopeptide was performed using the Paradigm MS4 HPLC system (Michrom BioResources). The fucosylated glycopeptides were dissolved in 25 μL of 0.1% formic acid, and 2 μL of the sample solution was injected into 2 μL capillary loop. The analytical column was a reversed-phase capillary column (Magic C18, 50 × 0.2 mm, 5 μm; Michrom BioResources). The mobile phase was 0.1% formic acid containing 2% acetonitrile (A buffer) and 0.1% formic acid containing 90% acetonitrile (B buffer). The fucosylated glycopeptides were eluted at a flow rate of 2 μL/min with a gradient of 5−65% of B buffer in 90 min.

Mass spectrometric analysis of fucosylated glycopeptides was performed using a FTICR/IT−MS (LTQ-FT; Thermo Fisher Scientific, Waltham, MA) equipped with a nanoelectrospray ion source (AMR, Tokyo, Japan). The conditions for FTICR−MS and IT−MS were as follows: an electrospray voltage of 2.0 kV in positive ion mode, a capillary temperature of 200 °C, a tube lens offset of 140 V, a collision energy of 35% for the MS^n experiment, maximum injection times (FTICR−MS and IT−MS) of 1250 and 50 ms, respectively, a resolution of FTICR−MS of 50 000, a scan time of approximately 0.2 s, dynamic exclusion of 18 s, and an isolation width of 3.0 u (range of precursor ion ±1.5).

First Run. The mass spectrometric mapping of fucosylated glycopeptides was performed by a sequential scan: full mass scan using FTICR−MS (*m*/*z* 1000−2000), data-dependent

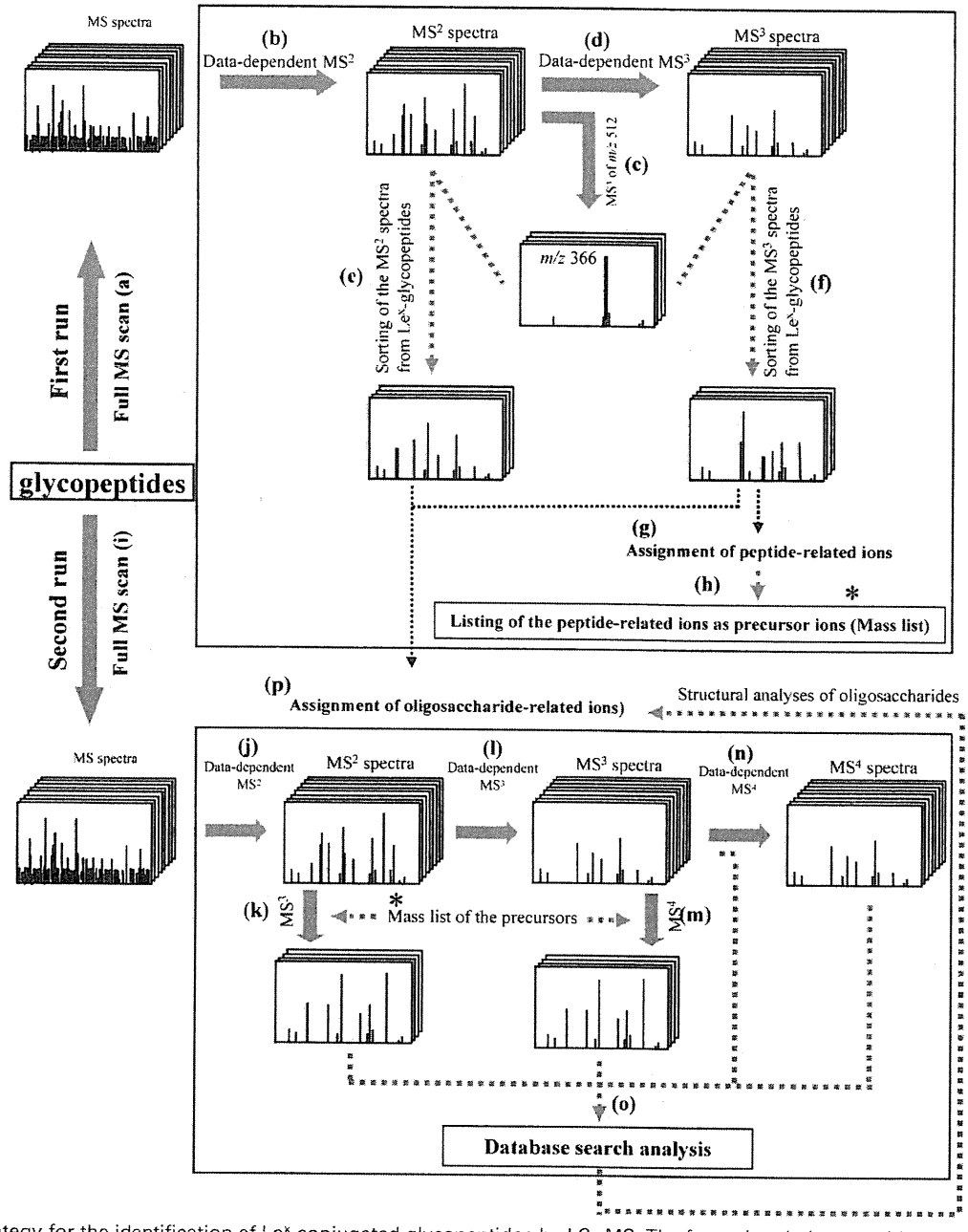

Figure 1. Strategy for the identification of Le^x-conjugated glycopeptides by LC–MS. The fucosylated glycopeptides were subjected to two different runs. In the first run, fucosylated glycopeptides were analyzed by (a) a full mass scan using the FTICR–MS, (b) data-dependent MS/MS, (c) MS/MS/MS of the Le^x-motif-distinctive ion (*m/z* 512), and (d) data-dependent MS/MS/MS. (e, f) On the basis of the presence of the product ion at *m/z* 512, which subsequently yielded the ion at *m/z* 366 by the MS/MS/MS, MS/MS and MS/MS/MS spectra of Le^x-conjugated glycopeptides were picked out from all the acquisition data. (g) Peptide-related ions were ascertained in the MS/MS/MS spectra. (h) The peptide-related ions were listed as precursor ions. In the second run, the fucosylated glycopeptides were identified by a full MS scan using the (i) FTICR-MS, (j) data-dependent MS/MS, (k) MS/MS/MS of the peptide-related ions listed as precursor ions, (l) data-dependent MS/MS/MS, (m) MS/MS/MS/MS of the peptide-related ions, and (n) data-dependent MS/MS/MS/MS. (o) Product ion spectra were submitted to database search analysis with a static modification of Cys with carboxymethyl (58.0 u) and possible modification of Asn with HexNAc (203.1 u) and dHex + HexNAc (349.1 u). MS^2, MS/MS; MS^3, MS/MS/MS; MS^4, MS/MS/MS/MS. (p) Carbohydrate structures were deduced from the oligosaccharide-related ions in the MS/MS and MS/MS/MS spectra.

MS/MS, MS/MS/MS of the Le^x-motif-distinctive ion (*m/z* 512) generated in data-dependent MS/MS, and MS/MS/MS of the most intense ions generated in data-dependent MS/MS by MS^n using IT–MS. Based on the presence of the product ion at *m/z* 512 that subsequently yielded the ion at *m/z* 366 by the MS/MS/MS, the MS/MS and MS/MS/MS spectra of expected Le^x-conjugated glycopeptides were picked out from all the acquisition data. Peptide-related ions were ascertained in the MS/MS/MS spectra, and were listed as precursor ions for the second run.

Second Run. Peptide sequencing was performed in a sequential scan: a full mass scan using FTICR−MS (*m/z* 1000−2000), data-dependent MS/MS, MS/MS/MS of the peptide-related ions listed as precursor ions, data-dependent MS/MS/MS, MS/MS/MS/MS of the peptide-related ions, and data-dependent MS/MS/MS/MS using IT−MS.

Protein Identification by Database Search Analysis. The spectra data obtained by the data-dependent collision-induced dissociation (CID)s and predominant CIDs of peptide-related ions were subjected to database search analysis with the TurboSEQUEST algorithm (BioWorks 3.1; Thermo Fisher Scientific) by using the NCBInr database (*Mus musculus*, 28−11−06). The static modification of carboxymethylation (58.0 u) at Cys, and the possible modification of HexNAc (203.1 u) and dHex + HexNAc (349.1 u) at Asn were used as the modified parameters of database search analysis. The SEQUEST criteria, known as cross correlation (Xcorr) scores, were set to 1.5/2.0/2.5 (charge states of +1/+2/+3) for the protein identifications. DTA files were generated for spectra with a threshold of 10 ions and a TIC of 100. Precursor and fragment ion mass tolerance in the MS^n spectra for database search analysis were set to 2.0 u and 1.0 u, respectively.

Results

Sorting out the Product Ion Spectra of the Le^x-Conjugated Glycopeptides by the First LC−MS/MS/MS Run. Proteins from mouse kidney cells were carboxymethylated and digested with trypsin. In the mass spectrometric mapping of the proteolytic digest, we often fail to acquire glycopeptide ions due to their lower ionization efficacy compared to coeluted unmodified peptides. To prevent interference by peptides in the ionization of glycopeptides, fucosylated glycopeptides including Lewis-motif-conjugated glycopeptides were enriched by affinity chromatography with an AAL-immobilized agarose column. The fucosylated glycopeptides were desalted by a C18 cartridge and injected into an LC−MS system equipped with FTICR−MS for a MS scan (*m/z* 1000−2000). The most intense ions on the MS scan were subjected to data-dependent MS/MS and MS/MS/MS, and an additional MS/MS/MS was performed when a dHex + Hex + HexNAc fragment (*m/z* 512) was detected on the MS/MS scan (Figure 1, first run). Figure 2A, B and C show the total ion chromatograms (TIC) obtained by the FTICR−MS scan of the fucosylated glycopeptides, the extracted ion chromatogram (EIC) of the dHex + Hex + HexNAc fragment acquired on the data-dependent MS/MS scan, and the EIC of the Hex + HexNAc fragment (*m/z* 366) that arose from the fragment at *m/z* 512 by the MS/MS/MS, respectively. We presumed that the Le^x-conjugated glycopeptides had been eluted around the peaks appearing in Figure 2C.

Assignments of the Peptide-Related Ions Derived from the Expected Le^x-Conjugated Glycopeptides. We picked out dozens of product ion spectra, and 22 precursors were determined to be the Le^x-conjugated glycopeptide-derived mass spectra based on the presence of Le^x-motif-distinctive ions. The elution positions of the glycopeptides are indicated in Figure 2C. In our previous report, most of the *N*-glycosylated peptides yielded peptide-related ions, such as [peptide + HexNAc + nH]$^{n+}$ and [peptide + (dHex)HexNAc + nH]$^{n+}$, which provided peptide fragment b- and y-ions by further CID, and subsequent database search analysis successfully revealed the peptide sequences of the glycopeptides.[27] In the present study, therefore, we examined the peptide-related ions in the product ion spectra of the glycopeptides 1−22 for peptide sequencing.

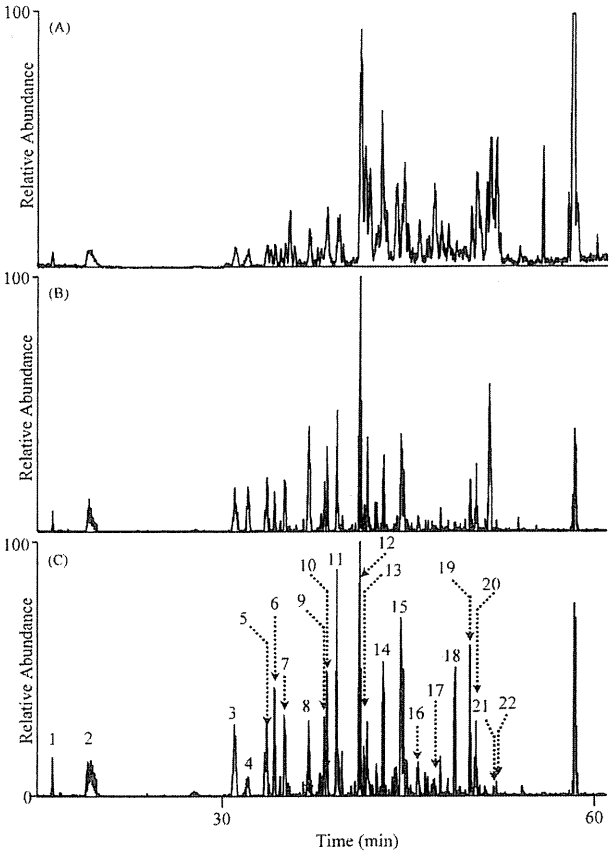

Figure 2. LC−MS^n of fucosylated glycopeptides. (A) Total ion chromatogram (TIC, *m/z* 1000−2000) of fucosylated glycopeptides. (B) Extracted ion chromatogram (EIC) of the ion at *m/z* 512 produced by data-dependent MS/MS. (C) EIC of the product ions at *m/z* 366 produced from the product ion at *m/z* 512 by MS/MS/MS. Expected Le^x-conjugated glycopeptides were designated as glycopeptides 1−22.

Figure 3A shows the integrated mass spectrum of the expected Le^x-glycopeptides eluted at 41−43 min. On the basis of an *m/z* spacing pattern that included *m/z* 67.69 ($HexNAc^{3+}$), *m/z* 54.02 (Hex^{3+}) and 48.69 ($dHex^{3+}$), intense ions at *m/z* 1067.105, 1134.803, 1189.505, and 1237.508 were assigned to triply charged ions of glycopeptides differing in glycosylation. Two intense ions, glycopeptides 12 (*m/z* 1237.508) and 13 (*m/z* 1134.803), were further subjected to MS/MS and MS/MS/MS, and yielded identical peptide-related ions at *m/z* 1650 (Figure 3B, C). This result indicates that glycopeptides 12 and 13 are glycoforms containing Le^x-motifs, and implies that the carbohydrate heterogeneity of a peptide of interest could be deduced from the integrated mass spectra.

Figure 4A indicates the MS/MS spectrum of glycopeptide 8. The presence of a dHex + Hex + HexNAc fragment (*m/z* 512) suggests that this glycopeptide is one of the Le^x-conjugated glycopeptides. The most intense fragment (*m/z* 1681.0) was further subjected to MS/MS/MS and provided a series of doubly charged Y-ions with an *m/z* spacing pattern, including *m/z* 101 ($HexNAc^{2+}$) and *m/z* 81 (Hex^{2+}). It was revealed that the fragment at *m/z* 906.2 was our desired product ion, [peptide + HexNAc + 2H]$^{2+}$ (Figure 4B).

Figure 5A and B show the MS/MS and MS/MS/MS spectra of glycopeptide 15, respectively. The triply charged ion (*m/z* 1414.4)

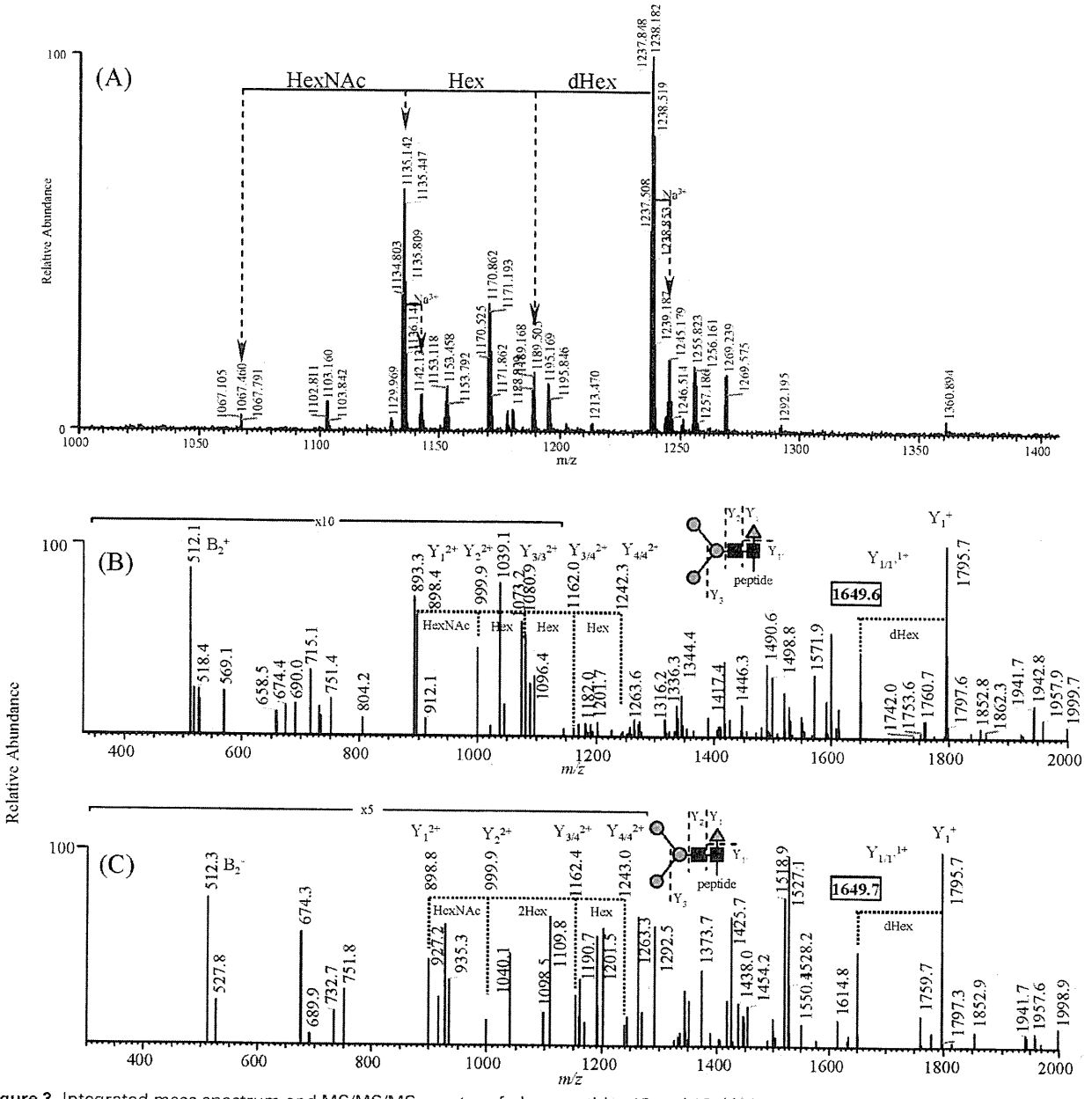

Figure 3. Integrated mass spectrum and MS/MS/MS spectra of glycopeptides 12 and 13. (A) Integrated mass spectrum of the expected Le^x-glycopeptides eluted at 41−43 min. (B) MS/MS/MS spectrum acquired from the most intense ion (*m/z* 1673.4) detected in the MS/MS spectrum of glycopeptide 12 (*m/z* 1237.8). (C) MS/MS/MS spectrum acquired from the most intense ion (*m/z* 1601.0) detected in the MS/MS spectrum of glycopeptide 13 (*m/z* 1135.4).

on the MS/MS scan was further subjected to MS/MS/MS and yielded a Y-ion series that included [peptide + 2HexNAc + 3Hex + dHex + 2H]$^{2+}$ (*m/z* 1764.3), [peptide + 2HexNAc + 2Hex + dHex+ 2H]$^{2+}$ (*m/z* 1683.5), [peptide + 2HexNAc + dHex + 2H]$^{2+}$ (*m/z* 1520.2), and [peptide + 2HexNAc + 2H]$^{2+}$ (*m/z* 1447.0). The fragment detected at *m/z* 1346.3 was assigned to our target ion, [peptide + HexNAc + 2H]$^{2+}$.

Alternative MS/MS and MS/MS/MS spectra of a Le^x-conjugated glycopeptide (glycopeptide 17) are shown in Figure 6A and B, respectively. The fragment at *m/z* 1515.4 on the MS/MS scan yielded Y-ion series that included [peptide + 2HexNAc + 3Hex + 2H]$^{2+}$ (*m/z* 1659.6), [peptide + 2HexNAc + 2Hex + 2H]$^{2+}$ (*m/z* 1578.3), and [peptide + 2HexNAc + 2H]$^{2+}$ (*m/z* 1416.5) on the MS/MS/MS scan. We deduced that the fragment at 1315.0 on the MS/MS/MS scan could be [peptide + HexNAc + 2H]$^{2+}$.

Finally we assigned out peptide + HexNAc, peptide + (dHex)HexNAc, and the peptide fragment from the product ion spectra of Le^x-conjugated glycopeptides 1−22 (Table 1). These peptide-related ions were listed as precursor ions in the second run, in which the listed ions were predominantly submitted to CID (Figure 1, second run).

Peptide Sequencing of the Expected Le^x-Conjugated Glycopeptides by the Second LC−MS/MS/MS/MS Run and Database Search Analysis. In the second run and subsequent database search analysis with modified parameters, including

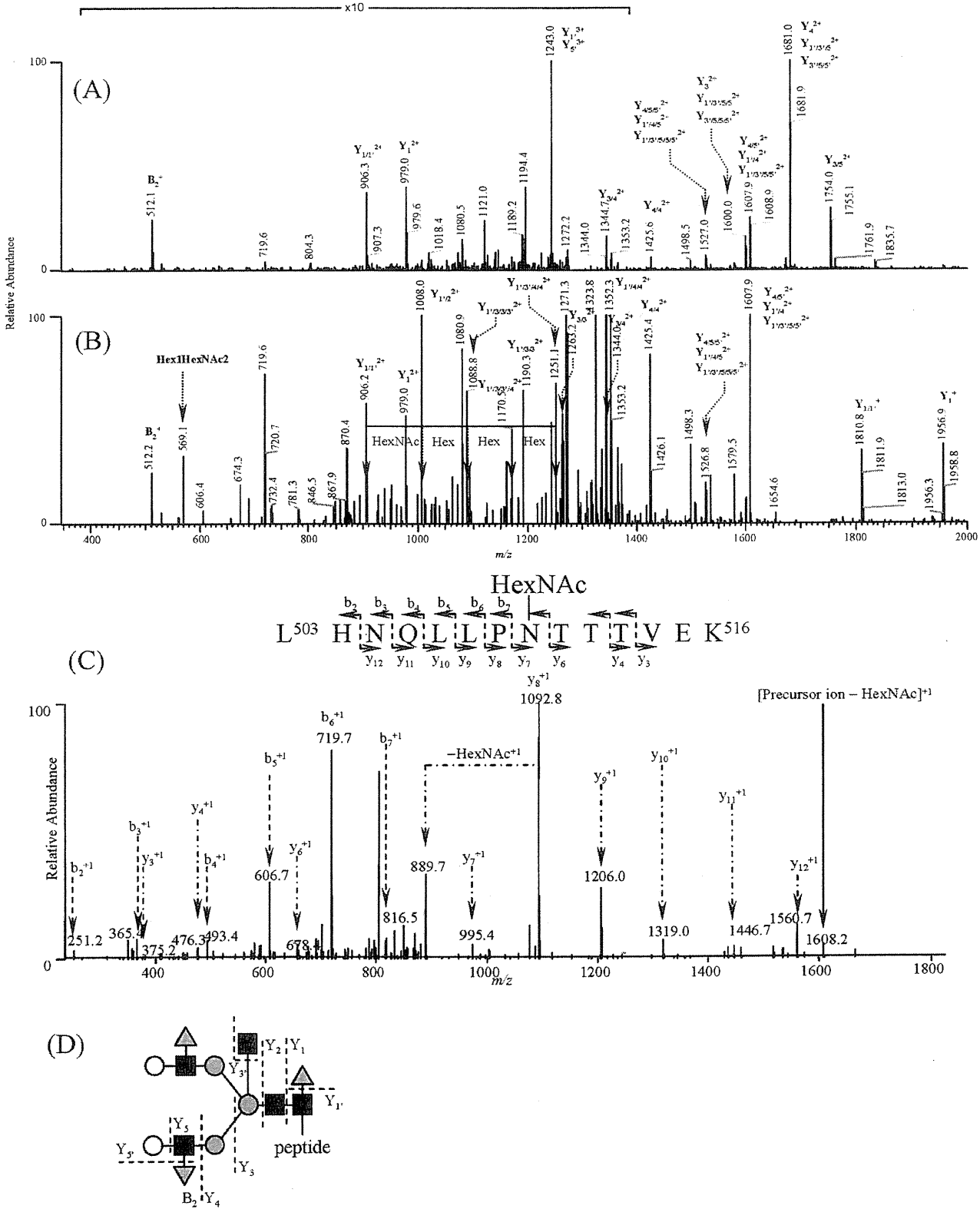

Figure 4. Identification of glycopeptide 8. (A) MS/MS spectrum acquired from the molecular ion $[M + 3H]^{3+}$ (*m/z* 1291.9) of glycopeptide 8 in Figure 2A. (B) MS/MS/MS spectrum acquired from the most intense ion (*m/z* 1681.0) in the MS/MS. (C) MS/MS/MS/MS spectrum acquired from the product ion (*m/z* 906.2) in the MS/MS/MS of glycopeptide 8, and amino acid sequence deduced from the results of database search analysis. (D) Deduced oligosaccharide structure. dHex, deoxyhexose; Hex, hexose; HexNAc, *N*-acetylhexosamine; white circle, galactose; gray circle, mannose; black square, *N*-acetylglucosamine; gray triangle, fucose.

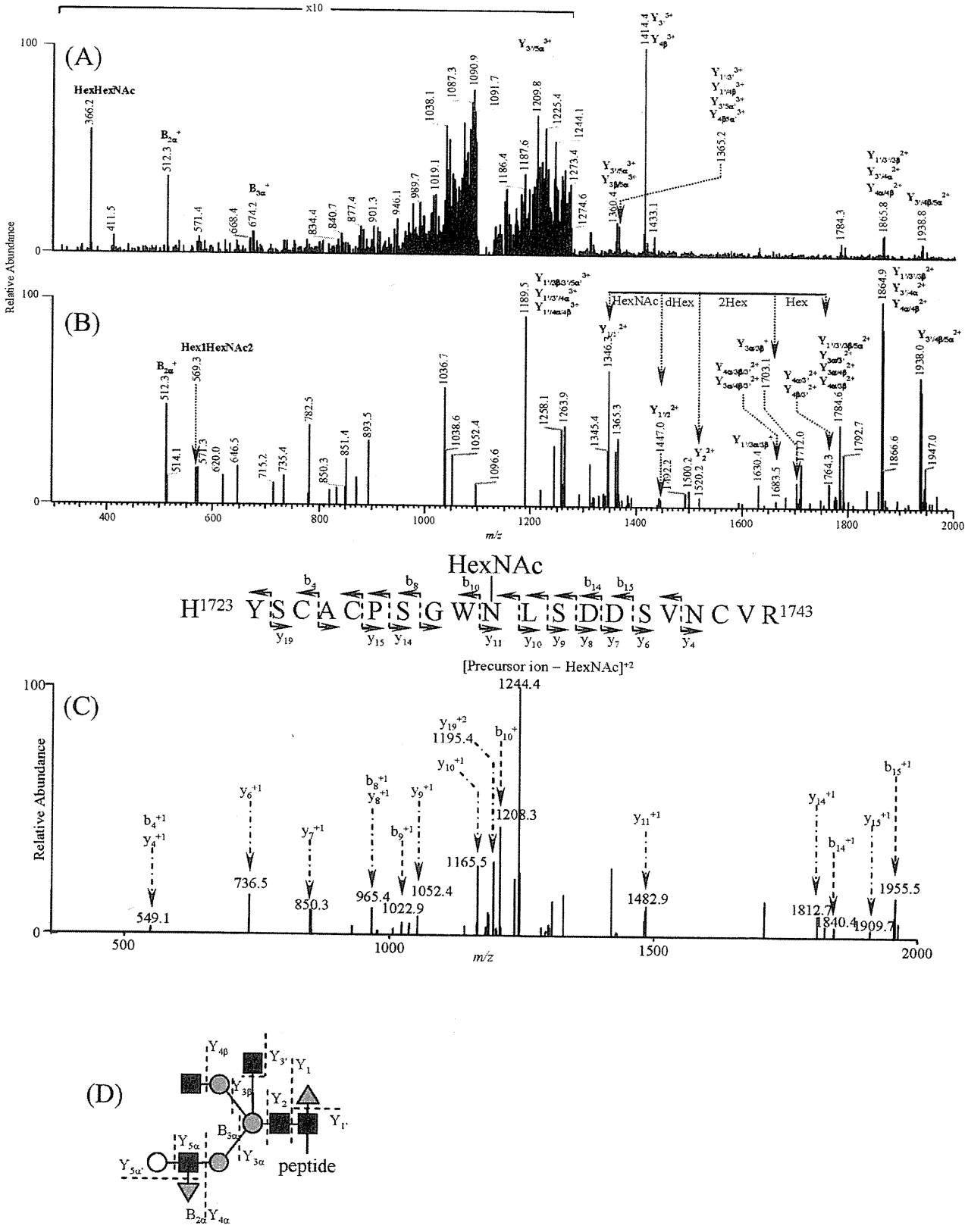

Figure 5. Identification of glycopeptide 15. (A) MS/MS spectrum acquired from the molecular ion $[M + 4H]^{4+}$ (*m/z* 1111.5) of glycopeptide 15 in Figure 2A. (B) MS/MS/MS spectrum acquired from the most intense ion (*m/z* 1414.4) in the MS/MS. (C) MS/MS/MS/MS spectrum acquired from the product ion (*m/z* 1346.3) in the MS/MS/MS of glycopeptide 15, and amino acid sequence deduced from the results of database search analysis. (D) Deduced oligosaccharide structure.

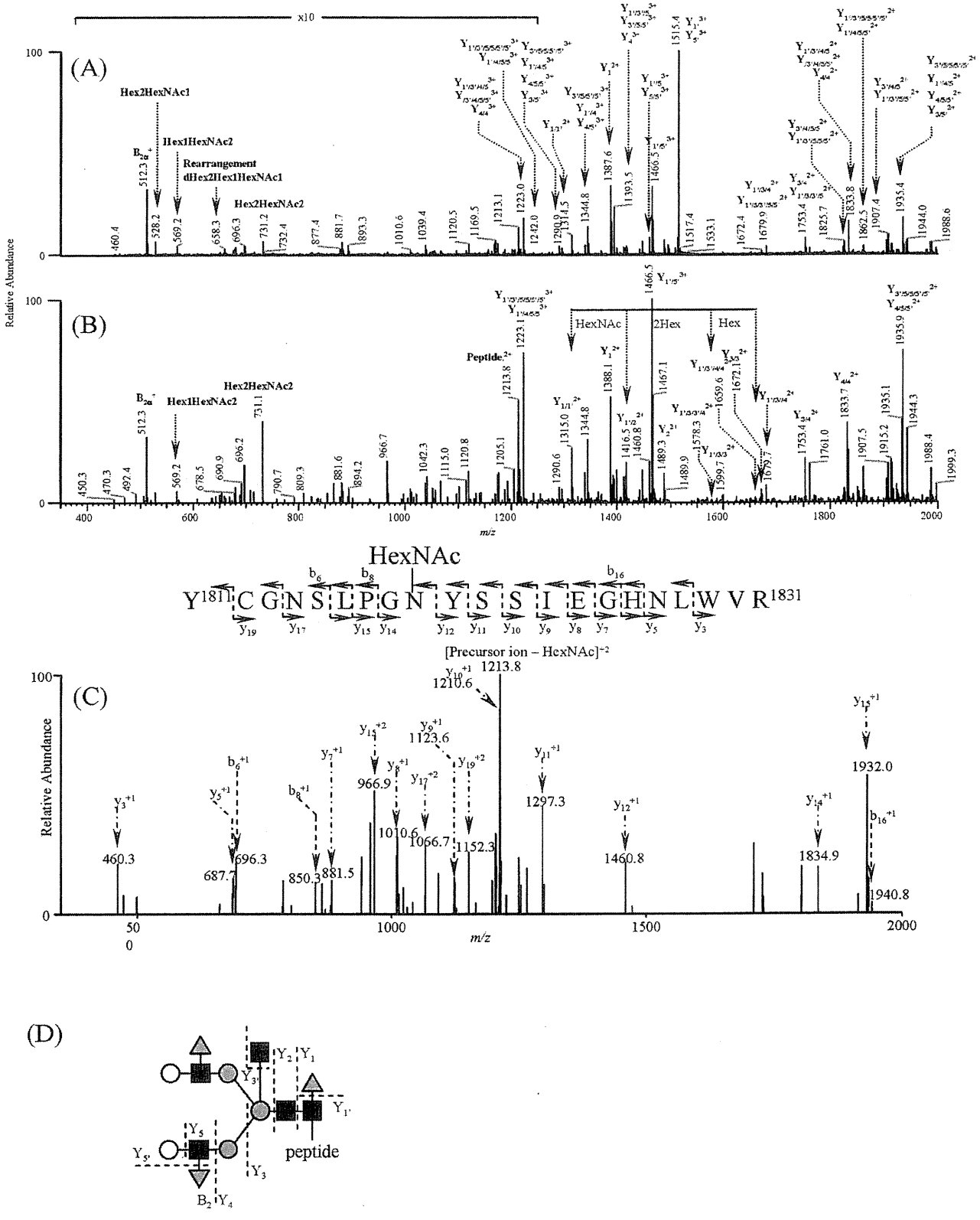

Figure 6. Identification of glycopeptide 17. (A) MS/MS spectrum acquired from the molecular ion $[M + 3H]^{3+}$ (*m/z* 1564.0) of glycopeptide 17 in Figure 2A. (B) MS/MS/MS spectrum acquired from the most intense ion (*m/z* 1515.4) in the MS/MS. (C) MS/MS/MS/MS spectrum acquired from the product ion (*m/z* 1315.0) in the MS/MS/MS of glycopeptide 17, and amino acid sequence deduced from the results of database search analysis. (D) Deduced oligosaccharide structure.

Table 1. Summary of Oligosaccharide Structures and Amino Acid Sequences of Le^x-Glycopeptides Detected by LC−MS^n and Database Search Analysis

	Candidate Le^x-glycopeptide					Peptide					Deglycosylated peptide prepared by PNGaseF-treatment				Oligosaccharide	
No	Observed *m/z* value of molecular-related ion[a]	Charge state	Observed *m/z* value of peptide-related ion[b]	Charge state	Additional sugar residue	Amino acid sequence	Xcorr[c]	Protein identified by database search analysis	GI no.[d]	Theoretical mass[e]	Calculated mass[f]	Observed *m/z* value of molecular-related ion[a]	Charge state	Xcorr[c]	Theoretical mass[g]	Calculated mass[f]	Deduced Structure	Theoretical mass[e]
1	1336.129	$[M+2H]^{2+}$	673.8	2	HexNAc	$E^{[69]}GN^{*}ATGHLMGR^{[80]}$	1.32	Cubilin precursor	88009268	1141.530	1141.530	572.280	2	2.53	1142.515	1142.845		2281.845
2	1170.147	$[M+3H]^{3+}$	1448.5	1	HexNAc	$N^{*[65]}LSYEAAPDHK^{[76]}$	1.52	cadherin 16	66472440	1243.583	1243.584	623.291	2	3.43	1244.567	1241.567		2281.845
3	1152.145	$[M+3H]^{3+}$	770.7	2	HexNAc+dHex	$R^{[23]}N^{*}WTETEVR^{[29]}$	3.33	dipeptidase 1	6981213	1189.584	1189.579	596.298	2	2.87	1190.568	1190.865		2281.845
4	1293.858	$[M+3H]^{3+}$	910.5	2	HexNAc	$Y^{[39]}YN^{*}QSAGGSHTFQR^{[51]}$	1.28	H-2 class I histocompatibility antigen, K-K alpha precursor	122159	1614.718	1614.717	808.865	2	4.19	1615.702	1615.715		2281.845
5	1225.510	$[M+3H]^{3+}$	1613.7	1	HexNAc	$T^{[445]}WSAFQN^{*}GTDKR^{[456]}$	1.32	low[-]density lipoprotein receptor-related protein 2 (LRP2)	124487372	1409.669	1409.673	471.227	3	1.66	1410.653	1410.659		2281.845
6	1122.805	$[M+3H]^{3+}$	807.7	2	HexNAc	$T^{[445]}WSAFQN^{*}GTDKR^{[456]}$	1.30	low[-]density lipoprotein receptor-related protein 2 (LRP2)	124487372	1409.669	1409.666	471.227	3	1.66	1410.653	1410.659		1973.735
7	1231.510	$[M+3H]^{3+}$	816.2	2	HexNAc	—[c]												
8	1291.243	$[M+3H]^{3+}$	906.2	2	HexNAc	$L^{[89]}IINQLLIN^{*}TTIVEK^{[104]}$	4.12	γ-glutamyltransferase 1 (γ-GTP1)	6679995	1696.868	1696.871	864.937	2	4.12	1697.852	1697.859		2281.845
9	1156.466	$[M+3H]^{3+}$	1079.0	3	HexNAc	$^{[242]}HHCELQN^{*}CSSTEFTCINSRPPNRR^{[266]}$	—	low[-]density lipoprotein receptor-related protein 2 (LRP2)	124487372	3002.281	3002.269	601.663	5	4.73	3003.265	3003.229		2793.035
10	1100.216	$[M+4H]^{4+}$	1170.0	2	HexNAc	$S^{[89]}GQEDHYWLDVEKN^{*}QSAK^{[104]}$	1.53	alanyl (membrane) aminopeptidase	225637483.00	2132.976	2132.976	—	—	—	—	—		2281.845
11	1123.900	$[M+5H]^{5+}$	915.6	3	HexNAc													
12	1233.506	$[M+3H]^{3+}$	1649.6	1	HexNAc	$N^{*[30]}MSSEFYATQLR^{[42]}$	1.73	γ-glutamyltransferase 1 (γ-GTP1)	6679995	1445.661	1445.660	724.340	2	3.78	1446.645	1446.665		2281.845
13	1134.803	$[M+5H]^{5+}$	1649.7	1	HexNAc	$N^{*[30]}MSSEFYATQLR^{[42]}$	1.30	γ-glutamyltransferase 1 (γ-GTP1)	6679995	1445.661	1445.664	724.340	2	3.78	1446.645	1446.665		1973.735
14	1163.044	$[M+4H]^{4+}$	1295.4	2	HexNAc	$V^{[1665]}VLVN^{*}FTHKPLDHIVLHPYR^{[1689]}$	1.29	low[-]density lipoprotein receptor-related protein 2 (LRP2)	124487372	2384.311	2384.312	796.118	3	4.73	2385.295	2385.332		2281.845
15	1111.553	$[M+4H]^{4+}$	1346.3	2	HexNAc	$H^{[1725]}YSCACPSGWN^{*}LSDDSVNCVR^{[1747]}$	2.82	low[-]density lipoprotein receptor-related protein 2 (LRP2)	124487372	2486.060	2486.059	—	—	—	—	—		1973.735
16	1145.460	$[M+4H]^{4+}$	1357.2	2	HexNAc	—	—	—	—	—	—	—	—	—	—	—		
17	1563.318	$[M+3H]^{3+}$	1315.0	2	HexNAc	$Y^{[1031]}CGNSLPGN^{*}YSSIEGDNLWVR^{[1053]}$	2.02	Cubilin precursor	[illegible]	2423.097	2423.098	—	—	—	—	—		2281.845
18	1481.528	$[M+2H+Na]^{3+}$	925.1	2	HexNAc	$Y^{[38]}GVTDVFPN^{*}GTQFSR^{[53]}$	—	Meprin A subunit beta precursor (endopeptidase-2)	2499913	1622.805	1622.573	812.903	2	3.14	1623.289	1623.791		2793.035
19	1156.990	$[M+4H]^{4+}$	1282.5	2	HexNAc	—	—	—	—	—	—	—	—	—	—	—		
20	1557.382	$[M+3H]^{3+}$	1204.5	2	non-substituted	$N^{*[67]}QSVVMYSVPQPLGHAHIPSR^{[89]}$	1.38	low[-]density lipoprotein receptor-related protein 2 (LRP2)	124487372	2405.289	2405.290	—	—	—	—	—		2281.845
21	1311.210	$[M+H+2Na]^{3+}$	924.9	2	HexNAc	$V^{[37]}GVTDVFPN^{*}GTQFSR^{[53]}$		Meprin A subunit beta precursor (endopeptidase-2)	2499913	1622.805	1622.810	812.903	2	3.14	1623.289	1623.791		2281.845
23	1386.270	$[M+3Na]^{3+}$	948.4	2	HexNAc	$Y^{[38]}GVTDVFPN^{*}GTQFSR^{[53]}$	—	Meprin A subunit beta precursor (endopeptidase-2)	2499913	1622.805	1622.928	812.903	2	3.14	1623.289	1623.791		2484.925

[a] Value obtained by FTICR−MS. [b] Value obtained by IT−MS^n. [c] Value of cross correlation obtained by database search analysis. [d] GenInfo Identifier number. [e] Monoisotopic value. [f] Value calculated by subtraction of the theoretical masses of deduced oligosaccharides from the observed monoisotopic masses of the candidate Le^x-glycopeptide. [g] Monoisotoic value. [h] No data. *, modification with HexNAc; #, modification with HexNAc+dHex. Bold portions of amino acid sequences, consensus sequences of -linked oligosaccharides.

possible modification at Asn with HexNAc (203.1 u) and with dHex + HexNAc (349.1 u), seven glycopeptides were successfully sequenced with a high cross-correlation score (charge +1, Xcorr > 1.5; charge +2, Xcorr > 2.0; charge +3, Xcorr > 2.5; charge +4, Xcorr > 3.0). Figure 4C shows the MS/MS/MS/MS spectrum acquired from glycopeptide 8 (precursor ion: [peptide + HexNAc + 2H]$^{2+}$, m/z 906.2). The database search analysis resulted in Leu^{503}-Lys^{516} in γ-glutamyl transpeptidase 1 (γ-GTP1) (charge +2, Xcorr: 4.12) (Table 1). The linkage of GlcNAc at Asn^{510} in the *N*-glycosylation consensus sequence, Asn-Thr-Thr, was suggested by the good agreement between the experimental b/y-ion pattern and the predicted pattern.

The MS/MS/MS/MS spectrum acquired from [peptide + HexNAc + 2H]$^{2+}$ (m/z 1346.3, glycopeptide 15) is shown in Figure 5C. This peptide was identified as His^{1723}-Arg^{1743} in low-density lipoprotein receptor-related protein 2 (LRP2, megalin) (charge +2, Xcorr: 2.82). The b- and y-ion pattern suggested the linkage of GlcNAc at Asn^{1733} in the *N*-glycosylation consensus sequence, Asn-Lys-Ser.

Figure 6C shows the MS/MS/MS/MS spectrum acquired from another expected Le^x-conjugated glycopeptide (glycopeptide 17; precursor ion: [peptide + HexNAc + 2H]$^{2+}$, m/z 1315.0). Database search analysis revealed that this peptide could be Tyr^{1811}-Arg^{1831} in the cubilin precursor (charge +2, Xcorr: 2.02) (Table 1). It was also suggested that the linkage position of GlcNAc was Asn^{1819} in the *N*-glycosylation consensus sequence of Asn^{1819}-Tyr-Ser^{1821}.

Glycopeptides 2, 10, 12, and 14 were also successfully identified as Asn^{519}-Lys^{529} in cadherin 16 (glycosylation site: Asn^{519}; charge +1, Xcorr: 1.52), Ser^{593}-Lys^{610} in alanyl (membrane) aminopeptidase (glycosylation site: Asn^{606}; charge +2, Xcorr: 1.53), Asn^{343}-Arg^{354} in γ-GTP1 (glycosylation site: Asn^{343}; charge +1, Xcorr: 1.73) and Val^{3444}-Lys^{3463} in LRP2 (glycosylation site: Asn^{3448}; charge +2, Xcorr: 1.79), respectively. Additionally, we deduced that glycopeptides 1, 3–6, 13, and 20 could be Le^x-conjugated glycopeptides from tolerable scores (charges +1 and +2 Xcorr > 1.30) (Table 1). All identified or probable glycopeptides contained consensus sequences of *N*-linked oligosaccharides.

By the present method, three glycoproteins were identified as proteins carrying multiple Le^x-conjugated oligosaccharides—namely, γ-GTP1 (glycosylation site: Asn^{343} and Asn^{519}; glycopeptides 8, 12 and 13), LRP2 (glycosylation site: Asn^{1497}, Asn^{1676}, Asn^{1733} and Asn^{3448}; glycopeptides 5, 6, 14, 15 and 20), and a cubilin precursor (glycosylation site: Asn^{1802}, Asn^{1819}, glycopeptides 1 and 17). Only one glycopeptide was sequenced, but it was deduced that cadherin 16, dipeptidase 1, H-2 class I histocompatibility antigen, and K–K alpha precursor (H2–K(k)), and alanyl (membrane) aminopeptidase could be the Le^x-conjugated glycoproteins.

The sequences of the Le^x-conjugated glycopeptides were confirmed by an additional LC–MS/MS of deglycosylated peptides prepared by PNGaseF-treatment. Because of the deamination of Asn residues by PNGase F treatment, we set the m/z values of [peptide + nH + 0.984 u monoisotopic mass]$^{n+}$ (n = 2–5) as precursor ions on the MS/MS. By this conventional method, 8 peptides that were sequenced by our method were identified as shown in Table 1. Moreover, two peptides which could not be sequenced by our method were also identified as His^{2943}-Lys^{2956} in LRP2 (glycopeptide 9), and Val^{540}-Lys^{554} in the meprin A β subunit precursor (endopeptidase-2, glycopeptides 18, 21 and 22). On the other hand, four glycopeptides that were sequenced by our method were not identified by the conventional method. Using both methods, we failed in the sequencing of four glycopeptides.

Structural Analyses of the Oligosaccharides in the Le^x-Conjugated Glycopeptides. The carbohydrate structures of the Le^x-conjugated glycopeptides were deduced from the fragment patterns and molecular masses obtained by the first run using FTICR-MS. The structural assignment of glycopeptide 8 is shown in Figure 4A and B. The carbohydrate composition was estimated to be 3dHex 5Hex 5HexNAc from the molecular mass of the carbohydrate moiety (calculated molecular mass of the glycan moiety: 2281.850). The fragment ions at m/z 1681.0 and m/z 1425.6 in Figure 4A were assigned to Y_4^{2+} and $Y_{4/4}^{2+}$, which arose from [M + 2H]$^{2+}$ (m/z 1681.8) by the dissociation of two molecules of the Lewis-motifs. The presence of B_2^+ (m/z 512) in both Figure 4A and B also suggested the binding of two Lewis-motifs. The Y_4^{2+} further yielded [Hex + 2HexNAc]$^+$ (m/z 569.1), $Y_{1'/3/3}^{2+}$ (m/z 1190.3) and $Y_{3/3}^{2+}$ (m/z 1263.2) on the MS/MS/MS, which suggested the presence of bisecting GlcNAc. The fucosylation of reducing-end GlcNAc was proven by the detection of $Y_{1/1}^{2+}$ ([peptide + HexNAc + 2H]$^{2+}$, m/z 906.2) and Y_1^{2+} ([peptide + dHex + HexNAc + 2H]$^{2+}$, m/z 979.0). Consequently, the glycan of glycopeptide 8 was characterized as a bisected and core-fucosylated oligosaccharide carrying two molecules of Le^x-motifs (Figure 4D). The possibility of the deduced structure was confirmed by the good agreement between the experimental mass (2281.850) and the theoretical mass (2281.845) (Table 1).

Figure 5A and B show the assignments of the carbohydrate moiety in the glycopeptide 15. The predominant ion (m/z 1414.4) in the MS/MS spectrum was assigned to [M – HexNAc + 3H]$^{3+}$ (Y_3^{3+} or $Y_{4/3}^{3+}$). This Y_3^{2+} ($Y_{4/3}^{3+}$) ion yielded the B_2^+ (m/z 512.3) by MS/MS/MS, suggesting the presence of only one molecule of the Lewis-motif. The presence of $Y_{1/1}^{2+}$ (m/z 1346.3), $Y_{1'/2}^{2+}$ (m/z 1447.0) and Y_2^{2+} (m/z 1520.2) suggested the fucosylation at the reducing end of GlcNAc. The presence of bisecting GlcNAc was deduced from the detection of the ion [Hex + 2HexNAc]$^+$ (m/z 569.3) and $Y_{1'3\alpha/3\beta}^{2+}$ (m/z 1630.4). From these fragments, the oligosaccharide structure was characterized as a bisected and core-fucosylated oligosaccharide carrying one molecule of the Le^x-motif (Figure 5D).

The deduced carbohydrate structure of glycopeptide 17 is indicated in Figure 6D. In the MS/MS spectrum, the fragments at m/z 1515.4 and m/z 1393.5 were assigned to [M – dHex + 3H]$^{3+}$ (Y_1^{3+} or Y_5^{3+}) and [M – dHex – Hex – HexNAc + 3H]$^{3+}$ (Y_4^{3+}), respectively (Figure 6A). The detection of B_2^+ (m/z 512.3) in both the MS/MS and MS/MS/MS spectra revealed the binding of two Le^x-motifs (Figure 6A and 6B). The presence of bisecting GlcNAc was suggested by the detection of the ion [Hex + 2HexNAc]$^+$ (m/z 569.2), $Y_{1'/3/3}^{2+}$ (m/z 1599.7) and $Y_{3/3}^{2+}$ (m/z 1672.1) in the MS/MS/MS spectrum (Figure 6B). The ions $Y_{1/1}^{2+}$ ([peptide + HexNAc + 2H]$^{2+}$, m/z 1315.0) and Y_1^{2+} ([peptide + dHex + HexNAc + 2H]$^{2+}$, m/z 1388.1) revealed the fucosylation at the reducing end of GlcNAc. We also found the presence of a distinctive ion of the Lewis y (Le^y) motif, (Fucα1–2)Galβ1–4(Fucα1–3)GlcNAc, at m/z 658.3 in the MS/MS spectrum. To determine whether *N*-linked oligosaccharides contained the Le^y-motif, *N*-linked oligosaccharides were released from mouse kidney proteins and treated with α1–2 fucosidase. Then the glycan profiles of the fucosidase-treated and -untreated oligosaccharides were compared by LC/MS. No change was found in the mass spectrometric glycan profiles between the two samples, but the fragment (m/z 658) was still detected in the MS/MS spectra of the enzyme-treated

glycopeptide 17 (data not shown). These results suggest the absence of α1−2 fucose on the glycopeptides. Consequently, we assigned the glycans of glycopeptide 17 to a bisected and core-fucosylated oligosaccharide carrying two Le^x-motifs (Figure 6D).

The oligosaccharide structures of other Le^x-conjugated glycopeptides were deduced from their B- and Y-type ions as well as the molecular masses obtained by FTICR−MS in the same manner (Table 1 and Figure 7). The most common structure was a bisected and fucosylated complex-type biantennary oligosaccharide carrying two Le^x-motifs (glycopeptides 1−5, 8, 10, 12, 14, 17, 20 and 21). A bisected and core-fucosylated complex-type biantennary oligosaccharide carrying one Le^x-motif was found in glycopeptides 6, 13, and 15. A bisected and core-fucosylated complex-type triantennary oligosaccharide carrying three Le^x-motifs was found in glycopeptides 9 and 18. The oligosaccharide structure of the glycopeptide in glycopeptide 22 was a triantennary carrying two Le^x-motifs. All experimental molecular masses of the deduced glycopeptides were identical to their theoretical masses (Table 1).

Discussion

Several glycan-epitopes, including Lewis antigens, HNK-1, and polysialic acid, have been widely shown to be involved in the physiological functions of glycoproteins and certain diseases. Some oligosaccharide-related antigens are being used as diagnostic markers of tumors in a clinical stage.[42,43] However, only a few proteins are known to carry the glycan-epitopes. To understand the physiological roles of the glycan-epitopes and to develop more effective diagnostic markers, we need methods that allow for the identification of target proteins carrying the glycan motif of interest. Glycan-epitopes are often detected by two-dimensional (2D)-electrophoresis in combination with lectin or immuno-blotting. The stained spots are subjected to in-gel tryptic digestion followed by protein identification by MS/MS and database search analysis. There are still problems in this procedure with the verification of the glycan structure in the identified protein. In addition, the procedure cannot be employed on hydrophobic membrane proteins having a high molecular weight.

In the present study, all proteins in the mouse kidney were digested into peptides, and the fucosylated glycopeptides were enriched by lectin-affinity chromatography. The resulting fucosylated glycopeptides were subjected to two different runs of LC−MS^n. In the first run, the elution positions of Le^x-conjugated glycopeptides in the tryptic peptide map were located based on the presence of Le^x-motif-distinctive ions. We picked out the product ion spectra of expected Le^x-conjugated glycopeptides from the elution positions and carefully assigned the peptide + HexNAc, peptide + (dHex)HexNAc, and peptide fragment. Then the fucosylated glycopeptides were subjected to a second run in which the peptide-related ions were set as precursor ions. We successfully identified γ-GTP1, LRP2, and the cubilin precursor as Le^x-conjugated glycoproteins by sequencing of 2−5 glycopeptides. Although only one glycopeptide was sequenced, cadherin 16, dipeptidase I, H2−K(k) and alanyl (membrane) aminopeptidase were characterized as Le^x-conjugated glycoproteins based on the good agreement between the experimental and theoretical masses of glycopeptides and their fragment patterns. Some of these were membrane proteins with high molecular masses over 400 kDa, the identification of which might have been difficult by 2D-electrophoresis with Western blotting.

Carbohydrate structures of the identified glycopeptides were deduced from the accurate molecular masses as well as fragment patterns obtained by the first run. We confirmed that all glycopeptides contained a bisected and core-fucosylated oligosaccharide carrying one or two molecules of Le^x-motifs at the *N*-linked oligosaccharide consensus sequence. Our model tissue was a mouse kidney in which we had previously confirmed the presence of Lewis x [Galβ1−4(Fucα1−3)GlcNAc] and/or y [(Fucα1−2)Galβ1−4(Fucα1−3)GlcNAc] motifs as well as the absence of Lewis a [Galβ1−3(Fucα1−4)GlcNAc] or b [(Fucα1−2)Galβ1−3(Fucα1−4)GlcNAc] motifs.[39] In this study, the Le^y-distinctive ions, (2dHex + Hex + HexNAc)$^+$ (*m*/*z* 658), were found in all MS/MS spectra of Lewis-conjugated peptides. However, treatment of α 1−2 fucosidase led to no change in the mass spectrometric glycan profile, suggesting the absence of the Le^y-motif. Recently, several groups have reported the internal migration of fucose residues in the ESI−CID of underived or derived carbohydrates.[44−48] Fucose residues are transferred between branches in liberated *N*-linked oligosaccharides by the ESI−CID.[49] Our finding suggests that the rearrangement of fucose residues also occurs by the ESI−CID of glycopeptides. This phenomenon makes it difficult to deduce the oligosaccharide structure from only the fragmentation pattern. A simultaneous use of lectins and/or antibodies would be crucial for the identification of the desired glycoproteins.

γ-Glutamyl transpeptidase 1 is associated with glutathione salvage, metabolism of endogenous mediators such as leukotrienes and prostaglandins. The attachment of Le^x-conjugated oligosaccharide to mouse γ-GTP 1 has already been demonstrated by Yamashita et al.[51] They determined the carbohydrate structures by the purification of γ-GTP 1 and the sequential exoglycosidase digestion in combination with methylation analysis. The oligosaccharide structures deduced from the MS/MS and MS/MS/MS spectra were in good agreement with those they reported. Furthermore, we revealed the heterogeneity of glycosylation on Asn^{343}.

Dipeptidase 1 is a glycosylphosphatidylinositol-anchored membrane glycoprotein. This protein is highly expressed in the kidney and small intestine and plays an important role in the degradation of cysteinyl-glycine, a glutathione produced by the removal of the glutamyl group from γ-glutamyl cysteinyl-glycine by γ-GTP.[52] The present study is the first report on the oligosaccharide structures of a mouse renal dipeptidase.

Cubilin, which is highly expressed in the renal proximal tubules, is a 460 kDa membrane glycoprotein consisting of 27 CUB (complement components C1r/C1s, Uegf, and bone morphogenic protein-1) domains. Cubilin is an endocytic receptor for intrinsic factor vitamin B12, albumin, apolipoprotein A-I, receptor-associated protein, immune globulin light chain and high-density lipoprotein.[50] These factors bind to cubilin through their CUB domains. The Le^x-conjugated oligosaccharides we found were all located on Asn^{1802} and Asn^{1819} in the CUB12 domain (Figure 8).

Low-density lipoprotein receptor-related protein 2, a high molecular weight membrane protein (520 kDa), is an endocytic receptor for several ligands, vitamin-binding proteins, apolipoproteins, hormones and enzymes. Cubilin and LRP2 are coexpressed in the renal proximal tubules and are associated with tubular protein reabsorption, vitamin metabolism and calcium homeostasis. Low-density lipoprotein receptor-related protein 2 consists of four ligand-binding sites containing cysteine-rich complement-type repeats and epidermal growth

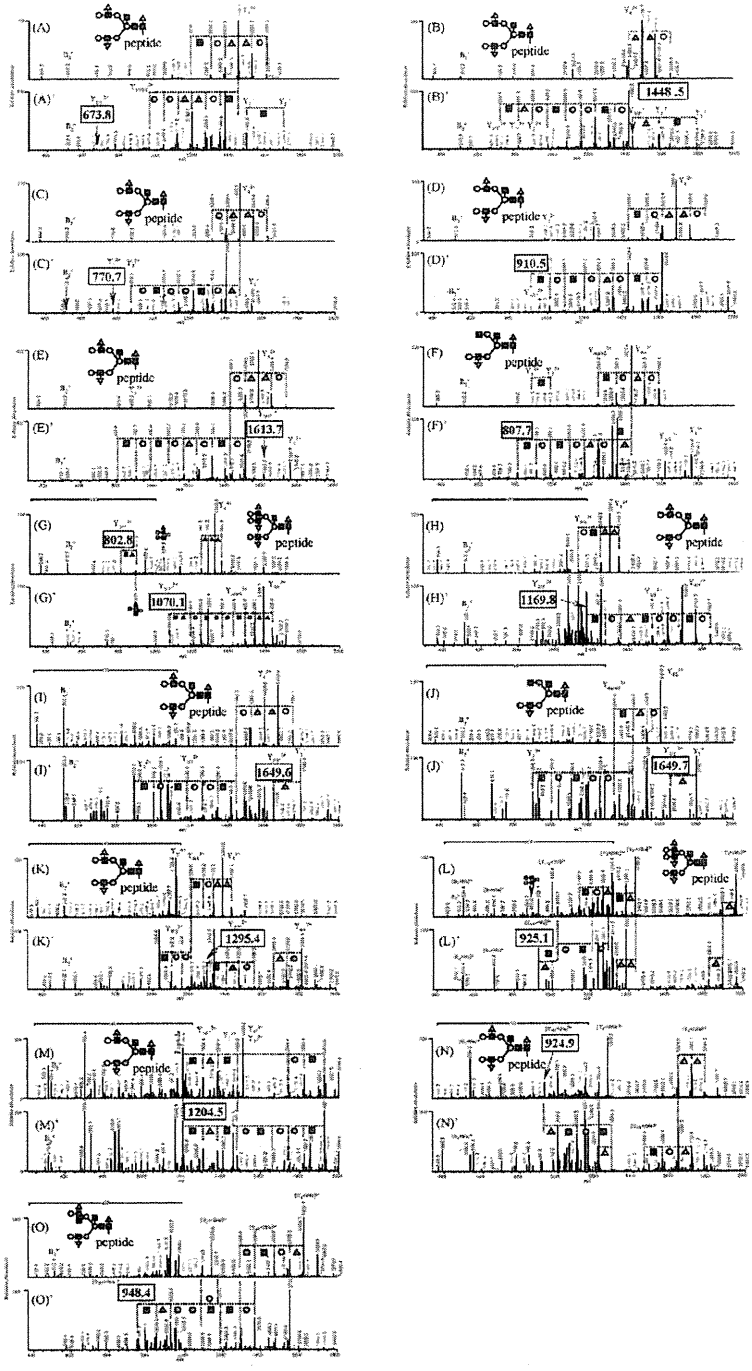

Figure 7. MS/MS and the MS/MS/MS spectra of glycopeptides 1−6, 9, 10, 12−14, 18 and 20−22, and deduced oligosaccharide structures. Boxed values are peptide-related ions. (A) MS/MS spectrum of the molecular ion (*m/z* 1136.4) of glycopeptide 1. (A′) MS/MS/MS spectrum of the predominant ion (*m/z* 1448.2) of (A). (B) MS/MS spectrum of glycopeptide 2 (*m/z* 1170.8). (B′) MS/MS/MS spectrum of the ion (*m/z* 1499.3) in (B). (C) MS/MS spectrum of glycopeptide 3(*m/z* 1152.5). (C′) MS/MS/MS spectrum of the ion (*m/z* 1472.5) in (C). (D) MS/MS spectrum of glycopeptide 4 (*m/z* 1294.2). (D′) MS/MS/MS spectrum of the ion (*m/z* 1685.0) in (D). (E) MS/MS spectrum of glycopeptide 5 (*m/z* 1226.0). (E′) MS/MS/MS spectrum of the ion (*m/z* 1582.6) in (E). (F) MS/MS spectrum of glycopeptide 6(*m/z* 1123.4). (F′) MS/MS/MS spectrum of the ion (*m/z* 1428.4) in (F). (G) MS/MS spectrum of glycopeptide 9 (*m/z* 1156.9). (G′) MS/MS/MS spectrum of the ion (*m/z* 1318.5) in (G). (H) MS/MS spectrum of glycopeptide 10 (*m/z* 1100.8). (H′) MS/MS/MS spectrum of the ion (*m/z* 1297.1) in (H). (I) MS/MS spectrum of glycopeptide 12 (*m/z* 1238.1). (I′) MS/MS/MS spectrum of the ion (*m/z* 1673.6) in (I). (J) MS/MS spectrum of glycopeptide 13 (*m/z* 1135.5). (J′) MS/MS/MS spectrum of the ion (*m/z* 1600.3) in (J). (K) MS/MS spectrum of glycopeptide 14 (*m/z* 1163.5). (K′) MS/MS/MS spectrum of the predominant ion (*m/z* 1380.8) in (K). (L) MS/MS spectrum of glycopeptide 18 (*m/z* 1482.6). (L′) MS/MS/MS spectrum of the predominant ion (*m/z* 1433.9) in (L). (M) MS/MS spectrum of glycopeptide 20 (*m/z* 1558.1). (M′) MS/MS/MS spectrum of the predominant ion (*m/z* 1509.8) in (M). (N) MS/MS spectrum of glycopeptide 21 (*m/z* 1279.2). (N′) MS/MS/MS spectrum of the predominant ion (*m/z* 1263.5) in (N). (O) MS/MS spectrum of glycopeptide 22 (*m/z* 1387.5). (O′) MS/MS/MS spectrum of the predominant ion (*m/z* 1825.5) in (O). White circle, galactose; gray circle, mannose; black square, *N*-acetylglucosamine; gray triangle, fucose.